

# Red Light-Triggered CO Release from $\text{Mn}_2(\text{CO})_{10}$ Using Triplet Sensitization in Polymer Nonwoven Fabrics

Sven H. C. Askes,<sup>†</sup> G. Uppendar Reddy,<sup>†</sup> Ralf Wyrwa,<sup>§</sup> Sylvestre Bonnet,<sup>\*,‡,§</sup> and Alexander Schiller<sup>\*,†,§</sup>

<sup>†</sup>Institute for Inorganic and Analytical Chemistry, Friedrich Schiller University Jena, Humboldtstraße 8, D-07743 Jena, Germany

<sup>‡</sup>Leiden Institute of Chemistry, Leiden University, Einsteinweg 55, 2333 CC Leiden, The Netherlands

<sup>§</sup>INNOVENT e.V. Technologieentwicklung Jena, Prüssingstraße 27 B, D-07745 Jena, Germany

## Supporting Information

**ABSTRACT:** Applicability of phototherapeutic CO-releasing molecules (photoCORMs) is limited because they are activated by harmful and poorly tissue-penetrating near-ultraviolet light. Here, a strategy is demonstrated to activate classical photoCORM  $\text{Mn}_2(\text{CO})_{10}$  using red light (635 nm). By mixing in solution a triplet photosensitizer (PS) with the photoCORM and shining red light, energy transfer occurs from triplet excited-state  $^3\text{PS}^*$  to a photolabile triplet state of  $\text{Mn}_2(\text{CO})_{10}$ , which, like under near-UV irradiation, led to complete release of carbonyls. Crucially, such “triplet-sensitized CO-release” occurred in solid-state materials: when PS and  $\text{Mn}_2(\text{CO})_{10}$  were embedded in electrospun nonwoven fabrics, CO was liberated upon irradiation with low-intensity red light ( $\leq 36$  mW 635 nm).

Although high concentrations of carbon monoxide (CO) are deadly to humans because it binds strongly to hemoglobin, CO is also a biological signaling molecule.<sup>1–3</sup> Controlled CO delivery has raised interest because it leads to positive effects on inflammation and wound healing, has a strong cell-protective action, can be used to eradicate microbes, and can relax smooth muscles to lower blood pressure.<sup>4–13</sup> However, delivering appropriate local concentrations of CO via respiratory administration is troublesome due to limited solubility of CO in human fluids and unintended systemic side effects.<sup>4,8</sup> These issues can be circumvented using a photoactive CO-releasing molecule (photoCORM) that releases CO upon light irradiation. The ability to deliver light locally and to tune light dose gives control over CO delivery location, timing, and dosage, while minimizing invasiveness of treatment.<sup>12</sup> Promising organic photoCORMs have been introduced by Wang et al.<sup>3,12,21,22</sup> However, photoCORMs are mostly inorganic coordination compounds, which can release one or more coordinated carbonyl ligands.<sup>1–3,10,14–22</sup> A disadvantage of most known photoCORMs is they can only be activated using ultraviolet or blue light.<sup>2,8</sup> Light in this region is not only toxic to cells and tissues,<sup>23,24</sup> but its penetration length through human skin and tissue is limited, typically not more than 1 mm.<sup>25,26</sup> Ideally, a clinician would better use red to near-infrared (NIR) light (phototherapeutic window: 600–950 nm), where light penetrates up to 10 mm in tissues.<sup>25</sup> Although work has shown molecular design and ligand tuning can shift the activation wavelength of photoCORMs toward the phototherapeutic window, it remains challenging to

obtain red light activation.<sup>2,10,11,14,20</sup> Moreover, many molecules activated at red-shifted wavelengths suffer from diminished CO-release efficiency, because less energy is provided to cleave the metal–carbonyl bond.<sup>2</sup> A strategy, presented by Ford et al., is to use lanthanoid-based upconverting nanoparticles (UCNPs) to upgrade 980 nm light to blue light that can be used to trigger CO release.<sup>2,15</sup> However, UCNPs require high excitation power ( $>1$  W) to deliver clinically relevant doses of blue light, which limits applicability.<sup>27,28</sup>

We discovered an approach to achieve CO-release with long-wavelength light at low power (Figure 1), which consists of

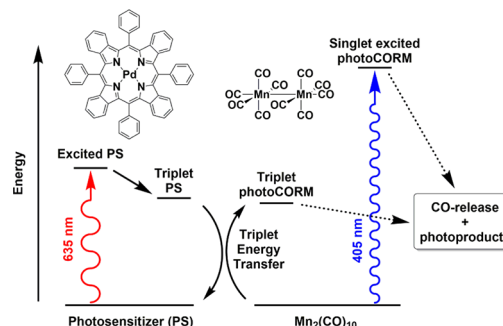


**Figure 1.** Triplet sensitization of  $\text{Mn}_2(\text{CO})_{10}$  with photosensitizer (PS), to achieve CO release using red light (635 nm, left side). Photochemical CO release can also be triggered with near-UV light excitation (405 nm, right side).

sensitizing the reactive triplet states of a classical photoCORM (i.e.,  $\text{Mn}_2(\text{CO})_{10}$ )<sup>1</sup> by using a triplet-state photosensitizer (palladium(II) tetraphenyltetrazoporphyryn; PS). In this scheme, PS absorbs a red photon to reach a singlet excited state that undergoes fast intersystem crossing to a long-lived triplet state (250  $\mu\text{s}$  in deoxygenated DMF).<sup>29</sup> The lifetime of this triplet state is long enough to allow collisions to occur with  $\text{Mn}_2(\text{CO})_{10}$ , transferring the triplet energy to the photoCORM. In its different triplet excited states, the photoCORM has electrons in anti bonding Mn–Mn or Mn–carbonyl bonds, which leads to Mn–Mn and Mn–CO bond dissociation, ultimately releasing CO.<sup>30</sup> This approach was proposed by Vogler in 1970<sup>31</sup> and Fox et al. in 1982<sup>32</sup> using blue light absorbing photosensitizers, with the underlying hypothesis higher wavelength

Received: July 17, 2017

Published: October 3, 2017

absorbing photosensitizers would not have enough energy in their triplet state to sensitize the triplet state of a CO-releasing molecule. We report this hypothesis was not correct, and CO release by  $\text{Mn}_2(\text{CO})_{10}$  can be sensitized using the red light absorbing sensitizer PS.

To follow photochemical release of CO in solution, PS and  $\text{Mn}_2(\text{CO})_{10}$  were dissolved in dimethylacetamide (DMA) and irradiated with red light (635 nm laser). The reaction was monitored via UV–vis absorption spectroscopy, direct detection of CO with a portable sensor, or liquid-phase infrared (IR) spectroscopy (Figure 2). The high-boiling point and weakly

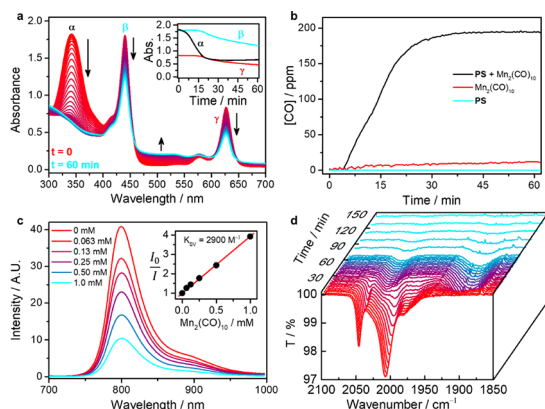


**Figure 2.** Photochemical release of CO using 635 nm light (150 mW) in a mixture of PS and  $\text{Mn}_2(\text{CO})_{10}$  in DMA. (a) Evolution of UV–vis absorption spectra in 1 min intervals during irradiation of a 3 mL solution ( $[\text{PS}] = 10 \mu\text{M}$ ,  $[\text{Mn}_2(\text{CO})_{10}] = 100 \mu\text{M}$ ). Inset: evolution of separate absorption bands at 340 nm ( $\alpha$ , black), 440 nm ( $\beta$ , blue), and 628 nm (red,  $\gamma$ ). (b) CO release vs time during irradiation of a 1 mL DMA solution in a closed desiccator setup. Black: mixture of PS (20  $\mu\text{M}$ ) and  $\text{Mn}_2(\text{CO})_{10}$  (1.0 mM). Red: only  $\text{Mn}_2(\text{CO})_{10}$ . Blue: only PS. (c) Phosphorescence of PS (10  $\mu\text{M}$ ,  $\lambda_{\text{exc}} = 635 \text{ nm}$ ) at different concentrations of  $\text{Mn}_2(\text{CO})_{10}$  in deoxygenated DMA. Inset: Stern–Volmer plot of data with a straight-line fit (slope =  $2900 \text{ M}^{-1}$ ,  $r^2 = 0.997$ ). (d) Evolution of liquid-phase IR-spectra during irradiation of a 1 mL DMA solution ( $[\text{PS}] = 200 \mu\text{M}$ ,  $[\text{Mn}_2(\text{CO})_{10}] = 10.0 \text{ mM}$ ). Spectra recorded every 3 min for the first 75 min, then every 15 min.

coordinating solvent DMA was chosen to avoid incompatibility of CO sensor with volatile organic solvents, and substitution of CO by solvent molecules. The UV–vis absorption spectrum before irradiation featured the superposition of the absorption of  $\text{Mn}_2(\text{CO})_{10}$  at 340 nm, originating from  $\sigma \rightarrow \sigma^*$  and  $d_{\pi} \rightarrow \sigma^*$  transitions in the Mn–Mn bond,<sup>30,35</sup> and the Soret and Q-bands of PS at 440 and 625 nm, respectively (Figures S4 and S6). Within 30 min of red light irradiation, absorption at 340 nm disappeared, indicating homolysis of the Mn–Mn bond and the concomitant formation of short-lived  $\text{Mn}(\text{CO})_5\cdot$  radicals.<sup>33</sup> Considering stoichiometry of the reaction (10  $\mu\text{M}$  PS and 100  $\mu\text{M}$   $\text{Mn}_2(\text{CO})_{10}$ ), it is photocatalytic. When PS was omitted and  $\text{Mn}_2(\text{CO})_{10}$  was irradiated with near-UV light (405 nm), the same evolution was observed (Figure S4). In absence of PS, no spectral evolution was observed for  $\text{Mn}_2(\text{CO})_{10}$  under red light irradiation (Figure S5). Thus, direct irradiation of  $\text{Mn}_2(\text{CO})_{10}$  with near-UV light and irradiation of a mixture of PS and  $\text{Mn}_2(\text{CO})_{10}$  with red light both led to photochemical breakage of the Mn–Mn bond.

To prove CO release during this photochemical reaction, a portable CO-sensor was embedded in a closed desiccator setup equipped with an optical fiber (Figure S3). During 60 min of red

light irradiation (635 nm, 150 mW) of a 1 mL solution of DMA containing 20  $\mu\text{M}$  PS and 1.0 mM  $\text{Mn}_2(\text{CO})_{10}$ ,  $195 \pm 13 \text{ ppm}$  of CO was reproducibly released in the desiccator (Figure 2, Figure S12), which corresponded on the one hand to 5.3 molecules of CO per molecule of  $\text{Mn}_2(\text{CO})_{10}$ , and on the other hand to an initial overall CO release quantum yield of 0.6% (Figure S12). Approximately the same amount of CO was released when a solution containing only  $\text{Mn}_2(\text{CO})_{10}$  was irradiated with near-UV light (405 nm, Figure S11), with 24% overall quantum yield. Furthermore, control experiments in which only  $\text{Mn}_2(\text{CO})_{10}$  or only PS was irradiated with red light did not result in CO-release (Figure 2b), and only slow release of CO was detected in the dark (Figure S13). Thus, these data present evidence CO is released after Mn–Mn homolysis using red light and PS.

To determine whether all carbonyls were released, photochemical reaction was followed by liquid-phase IR-spectroscopy using a silicon half-sphere attenuated total reflection (ATR) probe, on top of which photoreaction was carried out at 10-fold higher concentration (Figure 2d). This method made use of CO-stretch modes of  $\text{Mn}_2(\text{CO})_{10}$  in an otherwise vibrationally silent window between 1850 and 2200  $\text{cm}^{-1}$ . Within the first 30 min of irradiation, the three characteristic CO-stretches of  $\text{Mn}_2(\text{CO})_{10}$  at 2046, 2007, and 1983  $\text{cm}^{-1}$  disappeared. Meanwhile, two new bands appeared at 2022 and 1908  $\text{cm}^{-1}$ , which disappeared again in time. After 2 h of irradiation, the spectrum was flat, indicating loss of all ten carbonyls. An identical spectral evolution was observed when PS was omitted and  $\text{Mn}_2(\text{CO})_{10}$  was irradiated with near-UV light (405 nm, Figure S16). For both reactions, a brown precipitate indicated formation of  $\text{MnO}_2$ .<sup>34</sup> As only 5.3 CO were detected per molecule of  $\text{Mn}_2(\text{CO})_{10}$ , some processes must exist that produce disappearance of carbonyls without release of free CO. A recent report<sup>35</sup> indicated  $\text{O}_2$  may be involved, leading to release of  $\text{CO}_2$ . These data demonstrate direct excitation of  $\text{Mn}_2(\text{CO})_{10}$  with near-UV light and excitation of PS with red light in a mixture of PS and  $\text{Mn}_2(\text{CO})_{10}$ , leading to a reaction pathway in which all ten carbonyl ligands are released and  $\text{MnO}_2$  is formed.

CO-release from the photoCORM upon irradiation of PS is only conceivable when energy is intermolecularly transferred from the excited state of PS to  $\text{Mn}_2(\text{CO})_{10}$  upon diffusional collision. Because  $^1\text{PS}^*$  populates triplet state ( $^3\text{PS}^*$ ) within 6 ps after excitation,<sup>36</sup> spin conservation dictates energy transfer must lead to a triplet state in the energy acceptor. To obtain evidence for a triplet energy transfer mechanism, phosphorescence of PS was measured under deoxygenated conditions as a function of concentration of  $\text{Mn}_2(\text{CO})_{10}$  (Figure 2c). Phosphorescence intensity of PS at 800 nm ( $I$ ) decreased with increasing concentrations of  $\text{Mn}_2(\text{CO})_{10}$ , and a linear fit of  $I_0/I$  versus  $[\text{Mn}_2(\text{CO})_{10}]$  resulted in a Stern–Volmer quenching constant ( $K_{\text{SV}}$ ) of  $2900 \text{ M}^{-1}$ . These data confirmed triplet excited state of PS is quenched by  $\text{Mn}_2(\text{CO})_{10}$ . Considering unquenched lifetime ( $\tau_0$ ) of  $^3\text{PS}^*$  in DMF is 250  $\mu\text{s}$ ,<sup>29</sup> the quenching rate ( $k_q$ ) was  $1.2 \times 10^7 \text{ M}^{-1} \text{ s}^{-1}$ , lower than the diffusion-limited quenching rate in DMA ( $\sim 10^{10} \text{ M}^{-1} \text{ s}^{-1}$ ).<sup>37</sup> This shows only few collisions between  $^3\text{PS}^*$  and  $\text{Mn}_2(\text{CO})_{10}$  result in energy transfer, which may be the result of misalignment of the triplet-state energies. However, we also observed quenching of PS emission increased with red light exposure duration (Figure S9). This indicates the reaction intermediate(s) are better energy acceptor(s) than  $\text{Mn}_2(\text{CO})_{10}$ , which may in turn lead to additional CO-release. To the best of our knowledge, low-lying triplet states of  $\text{Mn}_2(\text{CO})_{10}$  around 1.5 eV (i.e., 800 nm) have never been reported and are neither absorbing nor emitting. It is known that

$\text{Mn}_2(\text{CO})_{10}$  triplet states are strongly dissociative,<sup>30</sup> and therefore their energy cannot be calculated easily. However, we note energy required to break the Mn–Mn bond, which was reported between 0.8 and 1.8 eV depending on the author,<sup>30</sup> is close to the triplet-state energy of PS (1.5 eV), so the energy transfer is in principle thermodynamically allowed. Our results support a diffusional quenching model in which the triplet excited-state energy of PS is transferred to  $\text{Mn}_2(\text{CO})_{10}$  upon collision (Figure 1). Compared to direct excitation of the UV band of  $\text{Mn}_2(\text{CO})_{10}$ , this method represents a red-shifting of the activation wavelength by more than 1.1 eV.

Because triplet-based reactions are highly oxygen-sensitive,<sup>38,39</sup> UV–vis absorption and CO-release experiments were repeated under deoxygenated conditions (30 min  $\text{N}_2$  bubbling). The UV–vis absorption band at 340 nm disappeared much quicker, i.e., within 5 min (Figure S8). This result can be interpreted by the fact the lifetime of PS is longer in absence of oxygen, leading to a higher quantum yield for energy transfer to  $\text{Mn}_2(\text{CO})_{10}$ . In contrast, slower CO-release was observed under deoxygenated conditions (Figure S14): about 2 h of irradiation was necessary to release all carbonyl ligands. This is in agreement with the fact oxygen is necessary to oxidize Mn(0) in the intermediate reaction products (e.g.,  $\text{Mn}(\text{CO})_5$ ) to release all carbonyls and form Mn(II/IV) oxides.<sup>34</sup> Because  $\text{N}_2$  bubbling in a solution never fully removes all traces of  $\text{O}_2$ , the reaction proceeded until completion. These data describe a double role for oxygen in this photoreaction: on the one hand,  $\text{O}_2$  competes with energy transfer; on the other hand, it is necessary for CO-release.

PhotoCORMs have potential as phototherapeutic compounds, but they should be immobilized in a carrier material to prevent release of potentially toxic metal fragments. Further, to facilitate diffusion-dependent triplet energy transfer, it is imperative PS and  $\text{Mn}_2(\text{CO})_{10}$  are mobile and in close proximity to each other. Electrospun nonwoven fabrics are attractive for phototherapeutic devices because they are easy to prepare, flexible, have high photoCORM loading capacity, and their high surface area allows quick photorelease of CO.<sup>16,34,40</sup> Thus, PS and  $\text{Mn}_2(\text{CO})_{10}$  were embedded in elastic nonwoven polymer fabrics using electrospinning of polycaprolactone (PCL, Figure 3a and Supporting Information). The resulting green-colored fabric (PCL-Mn-PS, Figure 3) was soft to the touch, flexible, and easy to cut and handle (Figure 3b). Control samples were made that contained only  $\text{Mn}_2(\text{CO})_{10}$  (PCL-Mn), only PS (PCL-PS),

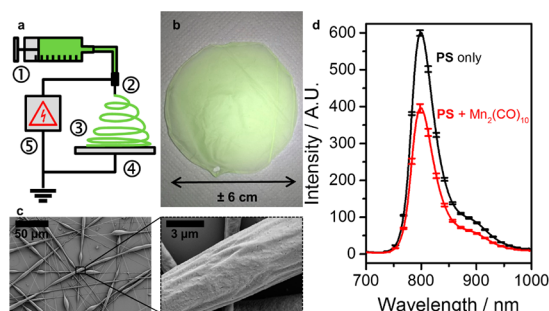


**Figure 3.** Synthesis and characterization of nonwoven fabric PCL-Mn-PS. (a) Schematic representation of electrospinning process. (1) syringe pump, (2) feed nozzle, (3) electrospun fiber, (4) collector plate, and (5) high voltage generator. (b) Photograph of PCL-Mn-PS. (c) SEM micrographs of PCL-Mn-PS. (d) Solid-state emission spectra of PCL-Mn-PS (red) and PCL-PS (black). Error bars represent standard deviation ( $N = 3$ ).

or neither (PCL). Optical microscopy and scanning electron microscopy (SEM) images confirmed fabrics consisted of randomly oriented fibers of 1–10  $\mu\text{m}$  diameter with a smooth surface (Figure 3c, Figures S19–S24). The solid-state emission spectrum of the fibers was recorded for PCL-PS and PCL-Mn-PS under 635 nm excitation, both showing the typical emission spectrum of PS at 800 nm (Figure 3d). Notably, the emission spectrum of PCL-Mn-PS was significantly less intense, at the same PS concentration, than that of PCL-PS. This is evidence the polymer matrix supports energy transfer from  $^3\text{PS}^*$  to  $\text{Mn}_2(\text{CO})_{10}$ .

To measure light-triggered CO-release from nonwoven fabrics, an adapted closed desiccator setup was used in which fabrics were carefully wrapped around the spherical diffuser tip of a medical-grade optical fiber, and irradiated in air with either 1.9 mW 405 nm or 36 mW 635 nm light (Figure 4).<sup>16,34</sup> Upon irradiation of

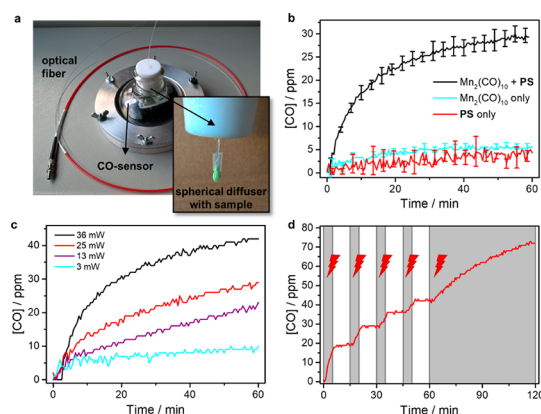


**Figure 4.** CO-release from nonwoven fabrics using red light (635 nm) in closed setup (a, details in Figure S3). The fabric (PCL-Mn-PS) is wrapped around the spherical diffuser tip. (b) Averaged CO-release as a function of red light irradiation time (36 mW) for samples PCL-Mn-PS (black), PCL-Mn (blue), and PCL-PS (red). Error bars represent standard deviation over 3 identical experiments. (c) CO-release from PCL-Mn-PS using red light irradiation at 36 mW (black), 25 mW (red), 13 mW (purple), and 3 mW (blue). (d) Red light irradiation of PCL-Mn-PS for 5 min intervals (gray), followed by 10 min darkness intervals (white).

PCL-Mn with near-UV light, rapid and reproducible CO-release was detected (Figure S26), which demonstrates the host material allows immediate escape of CO. Light-induced browning of the material indicated formation of  $\text{MnO}_2$  (Figure S27).<sup>34</sup> Then, red light induced CO-release was investigated with sample PCL-Mn-PS (Figure 4b). Rapid release of CO was observed, whereas red light irradiation of control samples PCL-PS and PCL-Mn resulted in no significant CO-release. Thus, both molecular compounds are needed for CO-release, like in solution (Figure 2b). Interestingly, after irradiation PCL-PS had bleached where it had been irradiated, i.e., it had turned white, whereas PCL-Mn-PS had browned, indicating  $\text{MnO}_2$  formation (Figure S28).<sup>34</sup> This result is in agreement with the observation that the emission of PS in PCL-Mn-PS was more stable than that of PS in PCL-PS (Figure S29), indicating greater photochemical stability of the sensitizer in the presence of the photoCORM acceptor. Meanwhile, SEM images of irradiated and nonirradiated parts of the sample showed no morphological changes due to irradiation (Figures S30 and S31). Our results confirmed PCL-Mn-PS released carbon monoxide upon red light irradiation via a triplet-sensitization mechanism.

The CO-release rate from PCL-Mn-PS could be tuned by varying irradiation intensity from 13 to 25 to 36 mW, which shows photorelease could be stimulated with lower light intensity. Higher intensity light caused melting of the polymer ( $T_{\text{melt}} = 60\text{ }^{\circ}\text{C}$ ). Furthermore, when red light irradiation was switched on and off (5 min irradiation, 10 min dark), CO-release from the nonwoven material was triggered “on-demand” (Figure 4d), whereas in solution the mixture was less responsive (Figure S15). Finally, the fabrics needed to be stored refrigerated and used within 10 days to prevent slow decomposition, probably of  $\text{Mn}_2(\text{CO})_{10}$ . Using more stable photoCORMs would solve these issues for future developments.

In conclusion, we showed how CO-release from  $\text{Mn}_2(\text{CO})_{10}$  could be sensitized under red light irradiation by mixing it with a commercially available photosensitizer (PS). Although very simple, this approach shifts the photorelease of CO from near-UV to the phototherapeutic window (635 nm), which represents a dramatic improvement over existing strategies. Photosensitization works not only in solution but also in solid-state nonwoven fabrics. Critically, CO release is obtained using low-intensity red light ( $\leq 36\text{ mW}$ ) and in air, in contrast to upconversion-based methods.<sup>15,38,39</sup> These findings open a new door to making potential devices for phototherapeutic CO delivery, for example for fabrication of red light responsive CO-releasing antibacterial or wound-healing bandages.

## ■ ASSOCIATED CONTENT

### Supporting Information

The Supporting Information is available free of charge on the ACS Publications website at DOI: 10.1021/jacs.7b07427.

Experimental details (PDF)

## ■ AUTHOR INFORMATION

### Corresponding Authors

\*alexander.schiller@uni-jena.de

\*bonnet@chem.leidenuniv.nl

### ORCID

Ralf Wyrwa: 0000-0003-4556-6510

Sylvestre Bonnet: 0000-0002-5810-3657

Alexander Schiller: 0000-0003-3888-8423

### Notes

The authors declare no competing financial interest.

## ■ ACKNOWLEDGMENTS

This work was supported by a grant from German Research Foundation (DFG) for supporting FOR 1738 (grant number SCHI 1175/2-2). A.S. thanks the DFG for a Heisenberg fellowship (grant numbers SCHI 1175/4-1 and SCHI 1175/5-1). ERC is acknowledged for a Starting grant to S.B. NWO is kindly acknowledged for financial support of S.B. via a VIDI grant.

## ■ REFERENCES

- (1) Motterlini, R.; Clark, J. E.; Foresti, R.; Sarathchandra, P.; Mann, B. E.; Green, C. J. *Circ. Res.* **2002**, *90*, e17.
- (2) Pierri, A. E.; Muizzi, D. A.; Ostrowski, A. D.; Ford, P. C. In *Luminescent and Photoactive Transition Metal Complexes as Biomolecular Probes and Cellular Reagents*; Lo, K. K.-W., Ed.; Springer Berlin Heidelberg: Berlin, Heidelberg, 2015; p 1.
- (3) Ji, X.; Damera, K.; Zheng, Y.; Yu, B.; Otterbein, L. E.; Wang, B. *J. Pharm. Sci.* **2016**, *105*, 406.
- (4) Heinemann, S. H.; Hoshi, T.; Westerhausen, M.; Schiller, A. *Chem. Commun.* **2014**, *50*, 3644.

- (5) Schatzschneider, U. *Eur. J. Inorg. Chem.* **2010**, *2010*, 1451.
- (6) Rimmer, R. D.; Richter, H.; Ford, P. C. *Inorg. Chem.* **2010**, *49*, 1180.
- (7) Ostrowski, A. D.; Deakin, S. J.; Azhar, B.; Miller, T. W.; Franco, N.; Cherney, M. M.; Lee, A. J.; Burstyn, J. N.; Fukuto, J. M.; Megson, I. L.; Ford, P. C. *J. Med. Chem.* **2010**, *53*, 715.
- (8) Schatzschneider, U. *Inorg. Chim. Acta* **2011**, *374*, 19.
- (9) Niesel, J.; Pinto, A.; N'Dongo, H. W. P.; Merz, K.; Ott, I.; Gust, R.; Schatzschneider, U. *Chem. Commun.* **2008**, 1798.
- (10) Chakraborty, I.; Carrington, S. J.; Mascharak, P. K. *Acc. Chem. Res.* **2014**, *47*, 2603.
- (11) Rimmer, R. D.; Pierri, A. E.; Ford, P. C. *Coord. Chem. Rev.* **2012**, *256*, 1509.
- (12) Wang, B.; Hu, L.; Siahaan, T. *Drug Discovery and Development*, 2 ed.; John Wiley and Sons: Hoboken, NJ, 2016.
- (13) Palao, E.; Slanina, T.; Muchová, L.; Šolomek, T.; Vitek, L.; Klán, P. *J. Am. Chem. Soc.* **2016**, *138*, 126.
- (14) Wright, M. A.; Wright, J. A. *Dalton Trans.* **2016**, *45*, 6801.
- (15) Pierri, A. E.; Huang, P.-J.; Garcia, J. V.; Stanfill, J. G.; Chui, M.; Wu, G.; Zheng, N.; Ford, P. C. *Chem. Commun.* **2015**, *51*, 2072.
- (16) Glaser, S.; Mede, R.; Gorls, H.; Seupel, S.; Bohlender, C.; Wyrwa, R.; Schirmer, S.; Dochow, S.; Reddy, G. U.; Popp, J.; Westerhausen, M.; Schiller, A. *Dalton Trans.* **2016**, *45*, 13222.
- (17) Reddy, G. U.; Axthelm, J.; Hoffmann, P.; Taye, N.; Gläser, S.; Görls, H.; Hopkins, S. L.; Plass, W.; Neugebauer, U.; Bonnet, S.; Schiller, A. *J. Am. Chem. Soc.* **2017**, *139*, 4991.
- (18) Diring, S.; Carne-Sanchez, A.; Zhang, J.; Ikemura, S.; Kim, C.; Inaba, H.; Kitagawa, S.; Furukawa, S. *Chem. Sci.* **2017**, *8*, 2381.
- (19) Sachs, U.; Schaper, G.; Winkler, D.; Kratzert, D.; Kurz, P. *Dalton Trans.* **2016**, *45*, 17464.
- (20) Kottelat, E.; Ruggi, A.; Zobi, F. *Dalton Trans.* **2016**, *45*, 6920.
- (21) Ji, X.; Zhou, C.; Ji, K.; Aghoghovbia, R. E.; Pan, Z.; Chittavong, V.; Ke, B.; Wang, B. *Angew. Chem., Int. Ed.* **2016**, *55*, 15846.
- (22) Ji, X.; Ji, K.; Chittavong, V.; Yu, B.; Pan, Z.; Wang, B. *Chem. Commun.* **2017**, *53*, 8296.
- (23) Hopkins, S. L. H.; Siewert, B.; Askes, S. H. C.; Veldhuizen, P.; Zwier, R.; Heger, M.; Bonnet, S. *Photochem. Photobiol. Sci.* **2016**, *15*, 644.
- (24) Wäldchen, S.; Lehmann, J.; Klein, T.; van de Linde, S.; Sauer, M. *Sci. Rep.* **2015**, *5*, 15348.
- (25) Vogel, A.; Venugopalan, V. *Chem. Rev.* **2003**, *103*, 577.
- (26) Plaetzer, K.; Krammer, B.; Berlanda, J.; Berr, F.; Kiesslich, T. *Lasers Med. Sci.* **2009**, *24*, 259.
- (27) Chen, Z.; Sun, W.; Butt, H.-J.; Wu, S. *Chem. - Eur. J.* **2015**, *21*, 9165.
- (28) Boyer, J.-C.; van Veggel, F. C. J. M. *Nanoscale* **2010**, *2*, 1417.
- (29) Vinogradov, S. A.; Wilson, D. F. *J. Chem. Soc., Perkin Trans. 2* **1995**, *0*, 103.
- (30) Rosa, A.; Ricciardi, G.; Baerends, E. J.; Stufkens, D. J. *Inorg. Chem.* **1996**, *35*, 2886.
- (31) Vogler, A. Z. *Naturforsch., B: J. Chem. Sci.* **1970**, *25*, 1069.
- (32) Fox, A.; Poe, A.; Ruminiski, R. *J. Am. Chem. Soc.* **1982**, *104*, 7327.
- (33) Perutz, R. N.; Torres, O.; Vlček, A., Jr. In *Comprehensive Inorganic Chemistry II*, second ed.; Poeppelemeier, K., Ed.; Elsevier: Amsterdam, 2013; p 229.
- (34) Bohlender, C.; Glaser, S.; Klein, M.; Weisser, J.; Thein, S.; Neugebauer, U.; Popp, J.; Wyrwa, R.; Schiller, A. *J. Mater. Chem. B* **2014**, *2*, 1454.
- (35) Li, Z.; Pierri, A. E.; Huang, P.-J.; Wu, G.; Iretskii, A. V.; Ford, P. C. *Inorg. Chem.* **2017**, *56*, 6094.
- (36) Jankus, V.; Snedden, E. W.; Bright, D. W.; Whittle, V. L.; Williams, J. A. G.; Monkman, A. *Adv. Funct. Mater.* **2013**, *23*, 384.
- (37) Montalti, M.; Credi, A.; Prodi, L.; Gandolfi, M. T. *Handbook of Photochemistry*, 3rd ed.; CRC Press: Boca Raton, FL, 2006.
- (38) Askes, S. H. C.; Pomp, W.; Hopkins, S. L.; Kros, A.; Wu, S.; Schmidt, T.; Bonnet, S. *Small* **2016**, *12*, 5579.
- (39) Balushev, S.; Katta, K.; Avlasevich, Y.; Landfester, K. *Mater. Horiz.* **2016**, *3*, 478.
- (40) Klinger-Strobel, M.; Gläser, S.; Makarewicz, O.; Wyrwa, R.; Weisser, J.; Pletz, M. W.; Schiller, A. *Antimicrob. Agents Chemother.* **2016**, *60*, 4037.